ELSEVIER

Polymer 41 (2000) 8909–8919

polymer

www.elsevier.nl/locate/polymer

Epitaxial crystallization and crystalline polymorphism of polylactides

L. Cartier[a,1], T. Okihara[a,2], Y. Ikada[b], H. Tsuji[c], J. Puiggali[a,3], B. Lotz[a,*]

[a]*Institut Charles Sadron, CNRS-ULP, 6 Rue Boussingault, 67083 Strasbourg, France*
[b]*Research Center for Medical Polymers and Biomaterials, Kyoto University, 53 Kawahara-cho, Shogoin, Sakyo-ku, Kyoto 606, Japan*
[c]*Department of Ecological Engineering, Faculty of Engineering, Toyohashi University of Technology, 1-1 Tempaku-cho, Toyohashi, Aichi 441, Japan*

Received 10 November 1999; received in revised form 1 February 2000; accepted 4 February 2000

Abstract

Two crystal phases of poly(L-lactide) and that of the racemate of poly(L-lactide) and poly(D-lactide) can be grown epitaxially on one and the same crystalline substrate, hexamethylbenzene (HMB), which had been shown by Zwiers et al. [Polymer 1983;24:167] to form a eutectic with these polymers. The stable α-crystal modification of the optically active polymer, based on a 10_3 helix conformation (for PDLA; 10_7 for PLLA), is obtained for T_c near 155°C. A new crystal modification is produced by epitaxial crystallization at slightly lower T_c (≈140°C). The crystal structure of this new form is established by electron diffraction and packing energy analysis. Two *antiparallel* helices are packed in an orthorhombic unit-cell of parameters $a = 9.95$ Å, $b = 6.25$ Å and $c = 8.8$ Å. The racemate of poly(L-lactide) and poly(D-lactide) also crystallize epitaxially (at ≈165°C) on HMB, which appears to be a very versatile substrate.

Keywords: Polylactide; Epitaxy; Crystal structure

1. Introduction

Polylactide, of formula $(O–CO–C{\cdot}H(CH_3))_n$, is the polyester equivalent of the polypeptide, polyalanine $(NH–CO–C^*H(CH_3))_n$. Since a heteroatom is present in the main chain (which has a chemical polarity), it is a genuine chiral polymer, the two enantiomers of which have been synthesized. It is of particular interest as a biocompatible material since it is metabolized to non-toxic compounds.

The optically active form is known to exist in two crystal structures with different helix conformations and cell symmetries. The conformation of the chain in the α-phase was determined by De Santis and Kovacs [1] to be a left-handed 10_7 helix for the L-isomer (PLLA), and a right handed 10_3 helix for the D-isomer (PDLA). Two chains are included in an orthorhombic unit-cell of parameters $a = 1.06$ nm, $b = 0.610$ nm and $c = 2.88$ nm. The ratio of a and b parameters, 1.737, is nearly equal to $\sqrt{3}$, indicating an almost hexagonal packing of helices. Several more recent investigations report slightly different parameters for the unit cell, but the detailed crystal structure has not been determined; Hoogsten et al. [2] observed extra 00*l* reflections which suggest some deviation from a "pure" 10_7 or 10_3 helix conformation. The second phase, hereafter the β-phase, was first observed in 1982 by Eling et al. [3] when investigating stretched fibers of PLLA. Its crystal structure has not yet been solved, although several investigations indicate that it is based on a three-fold helical conformation with a *c*-axis parameter of 0.88 nm[4] or 0.9 nm[2]. Hoogsten et al. [2] further suggest an orthorhombic unit cell ($a = 1.031$ nm, $b = 1.821$ nm) which houses *six* helices with, again, a near-hexagonal packing (the *b*/*a* ratio is 1.76, i.e. $\approx \sqrt{3}$); however, given the large size of the cell and number of helices, the detailed arrangement of the latter could not be worked out. More recently, Brizzolara et al. [5] made an extensive molecular modeling of the above structures and suggested, on the basis of data from Hoogsten et al., an orthorhombic unit cell with *two parallel* chains. As will be shown in the present and companion paper, the situation is more complex: there exist actually two distinct (but related) phases based on the three-fold helix conformation. The β-phase just considered is actually a *frustrated structure*, which has a trigonal cell with *three* chains in the cell (rather than six or two); the other, new phase introduced in the present paper (the γ-phase) turns out to be very close to

* Corresponding author. Tel.: +33-3-88-41-40-46; fax: +33-3-88-41-40-99.
E-mail address: lotz@cerbere.u-strasbg.fr (B. Lotz).
[1] Present address. ENSCL, Laboratoire GEPIFREM, Cité Scientifique, Bat C7 Av. Mendeleiev, BP108, 59652 Villeneuve d'Ascq, France.
[2] Permanent address. Department of Applied Chemistry, Faculty of Engineering, Okayama University, Okayama 700, Japan.
[3] Permanent address. ETSEIB, Department d'Enginyera Quimica, Diagonal, 647 E-08028 Barcelona, Spain.

0032-3861/00/$ - see front matter
PII: S0032-3861(00)00234-2

the model proposed by Brizzolara et al. for the β-phase: it has an orthorhombic unit-cell that houses two *antiparallel* helices.

The racemic blend of polylactides forms a crystal structure which is known [6] to have a melting temperature (220°C) significantly higher than those of the enantiomeric α- or β-forms (185 and 175°C, respectively), in spite of very similar or (for the latter structure) even identical helix conformations. Following the initial work of Ikada et al. [6] a crystal structure has been proposed for the racemate by Okihara et al. [4]. The unit-cell is triclinic (space group $P\bar{1}$) with parameters $a = b = 0.916$ nm, $c = 0.89$ nm, $\alpha = \beta = 109°2$, $\gamma = 109°8$ and houses two enantiomorphous helices. In several recent works (Okihara et al. [4,7], Brizzolara et al. [5] and Cartier et al. [8]), the racemate was observed to produce highly unconventional single crystals with *triangular* morphology. As shown by Cartier et al. [8] this morphology results from differences in growth rates on opposite sides of the (110) growth planes, which reflect differences in molecular characteristics and/or concentrations of the co-crystallizing enantiomeric species: for identical M_w and concentrations, hexagonal single crystals are formed [8]. These authors also pointed out that the unit cell considered by Okihara et al. [5] is a subcell of a larger trigonal cell that includes *six* three-fold helices, with parameters $a = b = 1.498$ nm, $c = 0.87$ nm and symmetry $R3c$ or $R\bar{3}c$. This unit cell is more familiar for chiral but racemic *homopolymers*, in particular isotactic polyolefins (poly(1-butene) [9], polystyrene [10], etc.) which can adopt either right- or left-handed helical conformations. By contrast, the unit cell of the polylactide racemate houses of course *two different* (*enantiomeric*) *molecular species*.

In a different context, Zwiers et al. [11] have reported that blends of polylactides and hexamethylbenzene [12] (HMB) form eutectics, with the eutectic composition at 65% concentration of PLLA. Scanning electron micrographs obtained after removal of the HMB solvent–substrate indicate oriented growth of the polymer upon solidification of HMB-rich mixtures. In line with several earlier observations made on binary polymer–crystallizable solvent systems [13,14], these results suggest that upon solidification of the eutectic the polymer crystallizes epitaxially on the freshly formed substrate crystals.

We report in this paper on the epitaxial crystallization of polylactides (both enantiomers and racemates), and on its use in a further investigation of their crystal structures and polymorphism. Rather surprisingly, three crystal phases of polylactides have been epitaxially crystallized on HMB, which turns out to be a highly versatile substrate. These are: (1) the racemate; (2) the "standard" α-phase of the enantiomer (based on 10_3 or 10_7 helices); and (3) an original modification, referred to hereafter as the γ-phase. This phase has been obtained so far only by epitaxial crystallization; its structure is actually very close to a model proposed by Brizzolara et al. [5] for the "stretched" β-form. In a companion paper [15], we deal specifically with this "stretched" β-phase of PLLA, which is *not* obtained by epitaxial crystallization, and which rests on a recently uncovered *frustrated packing scheme* [16,17] that applies frequently (but not exclusively [18]) for polymers with three-fold helical symmetry.

2. Experimental

The synthesis of the poly(L-lactide) and poly(D-lactide) has been described in detail [19]. The samples have been used in numerous investigations on the structure and morphology of triangular single crystals, and on the properties of enantiomeric and racemic polylactides [4,7,20–25]. Several samples were used during this study, but mainly a couple of enantiomers with identical, 7000 molecular weight. Since, however, the structural features discussed in the present study do not depend on molecular weight, the latter will not be quoted further.

HMB (mp: 166–168°C) is of commercial origin (Sigma Aldrich Fluka) and is used without further purification.

The sample preparation and experimental procedures have been described on various occasions [26]: a thin film of polylactide (typically in the 10–50 nm range) is cast on a glass coverslide by evaporation of a dilute solution in *p*-xylene or methylene chloride. A small amount of HMB (the crystal structure of which is known [12]) is deposited on a glass slide, which is covered with the coverslide with the PLA film. The sandwich is left on a hot (≈180°C) surface (for example, a Kofler bench). The HMB sublimes and condenses on the cooler coverslide, producing sufficiently large single crystals (up to several tens of μm). The slide and coverslides are then transferred to the crystallization temperature. As performed here, the experiment is rather touchy, since the melting temperatures of the materials and substrate are very close. For the racemic blends at least, but also for the enantiomers, it is probable that the depositing crystals of HMB initially dissolve the polymer. This unusual procedure was used to spare the polymer, in limited supply. As judged from the results of Zwiers et al. a

Fig. 1. (a) Epitaxial crystallization of PLLA on a single crystal of HMB produced by sublimation. The PLLA of the film produces small spherulites. Optical microscopy, phase contrast. Scale bar: 25 μm. (b) Electron diffraction pattern of an epitaxially crystallized film as in (a). Chain axis vertical. (c) Indexation of the diffraction pattern in (b), assuming a 10_7 helical conformation of PLLA and an orthorhombic unit-cell (cf. Part (d)). The *bc*-plane is the contact plane in the epitaxy. (d) *hk*0 electron diffraction pattern obtained from solution-grown single crystals of the α-phase of PLLA. *a*-axis horizontal, *b*-axis vertical (cf. Ref. [8]). (e) Representation of the α-phase of PLLA assuming regular 10_7 helix conformation and parallel helices. This model is an oversimplification of the actual crystal structure.

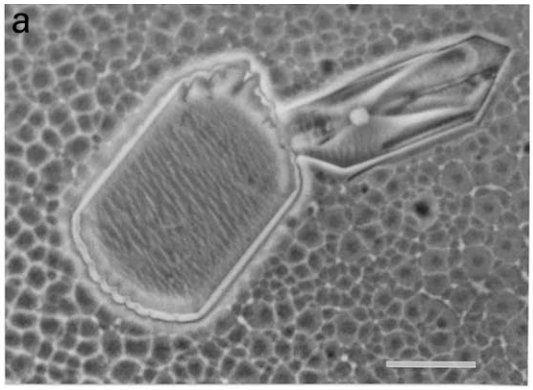
a

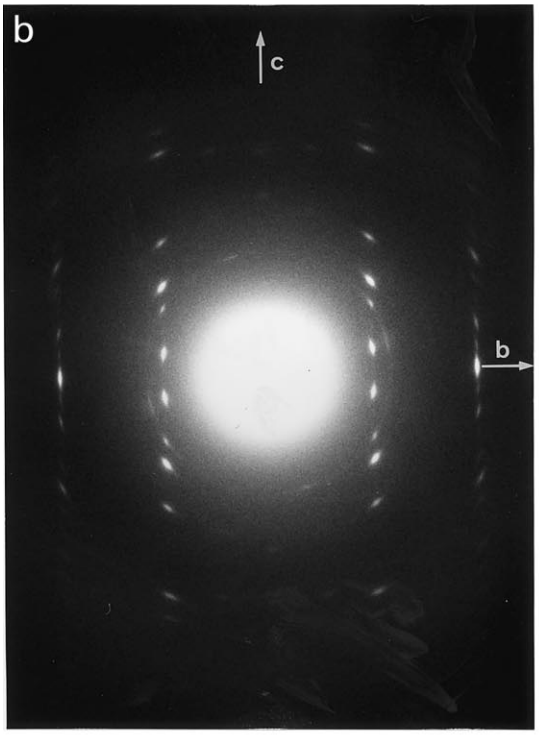
b
c
b

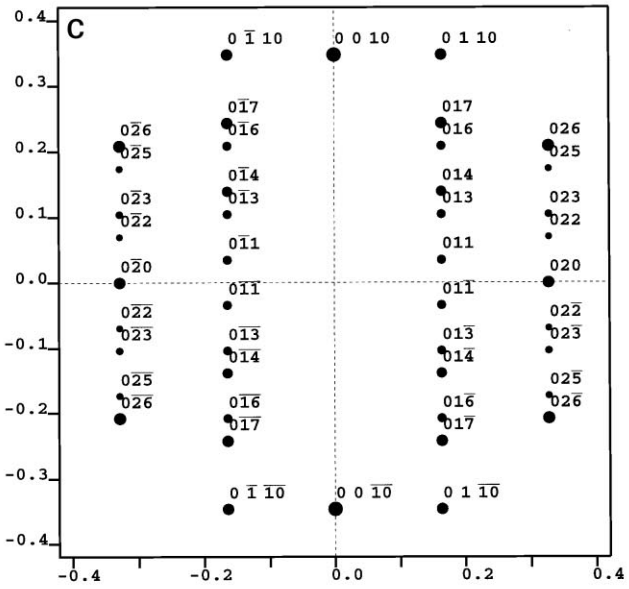
c
0 1̄ 10
0 0 10
0 1 10
0 1̄ 1̄0
0 0 1̄0
0 1 1̄0
0.4
0.3
0.2
0.1
0.0
-0.1
-0.2
-0.3
-0.4
-0.4
-0.2
0.0
0.2
0.4

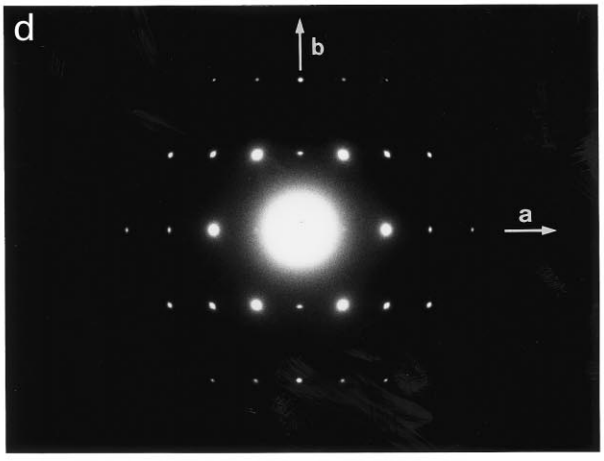
d
b
a

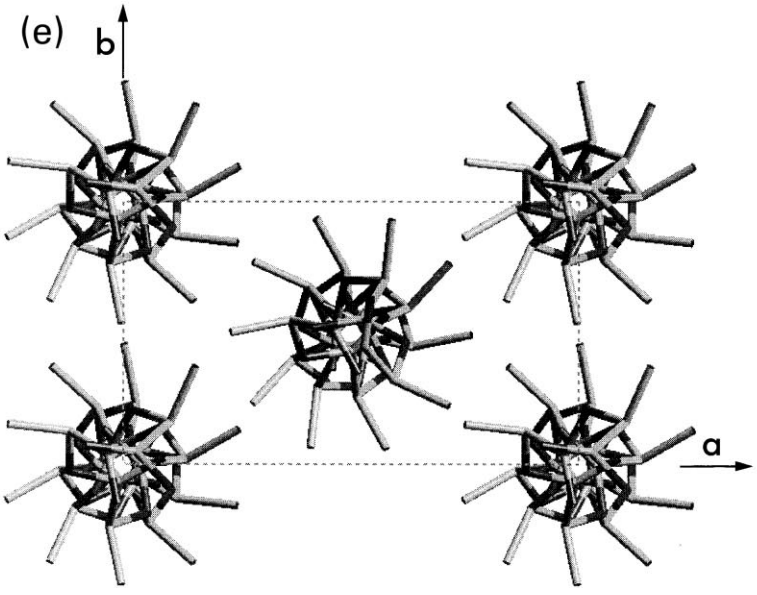
(e)
b
a

more conventional co-melting and crystallization would be equally valid. After cooling, the glass slides are separated, and the HMB crystals are dissolved in acetone, a non-solvent of the polymer. The exposed polymer film is then processed for observation by electron microscopy: shadowed with Pt/C (when desired), backed with a carbon film, floated off on water (sometimes with the help of a polyacrylic acid backing) and deposited on electron microscope support grids.

The samples are examined in a Philips CM12 electron microscope operated at 120 kV. Molecular modeling is performed with the relevant packages and the standard potentials developed by Biosym-Molecular Simulations (Cambridge, UK and Waltham, MA).

3. Results and discussion

3.1. Epitaxy of three crystal phases of polylactides on HMB

A surprising outcome of the present investigation is that *two* crystalline modifications of the polylactides (plus the racemate) could be produced by epitaxial crystallization on a *single* substrate, namely HMB. The relevant variable is the crystallization temperature. As already indicated, the crystal phases of enantiomeric and racemic polylactides have significantly different melting temperatures, ranging from 175 and 185°C for the enantiomeric β- and α-phases to 230°C for the racemate. Crystallization ranges follow the same pattern. The optically active form crystallizes at rather low temperatures, as expected from its lower melting temperature: the α-phase is obtained at 155°C, whereas a new, γ-phase (but *not* the anticipated β-phase) is formed at 140°C. In our experiments, the racemate is commonly obtained for crystallization temperatures very near the melting temperature of HMB, i.e. 165°C. We present now the diffraction evidences gathered on the epitaxially crystallized films of these three crystal forms, before deriving the crystal structure of the newly observed γ-phase.

3.1.1. α-Phase epitaxy

Epitaxial crystallization of PLLA on HMB at 155°C yields a polymer film with single chain axis and lamellar orientations (Fig. 1a). The corresponding diffraction pattern (Fig. 1b) has a complex layer line structure, which suggests at once the stable crystal modification of PLLA based on a 10_7 helical conformation (or 10_3 for PDLA), in agreement with the conclusions of De Santis and Kovacs [1]. Using the unit-cell parameters determined by Hoogsten et al. [2] (a = 1.07 nm, b = 0.595 nm, c = 2.78 nm) or the slightly different ones redetermined in the present investigation (a = 1.06 nm, b = 0.610 nm, c = 2.88 nm), it is an easy matter to show that the contact plane is the *bc*-plane: indeed, the

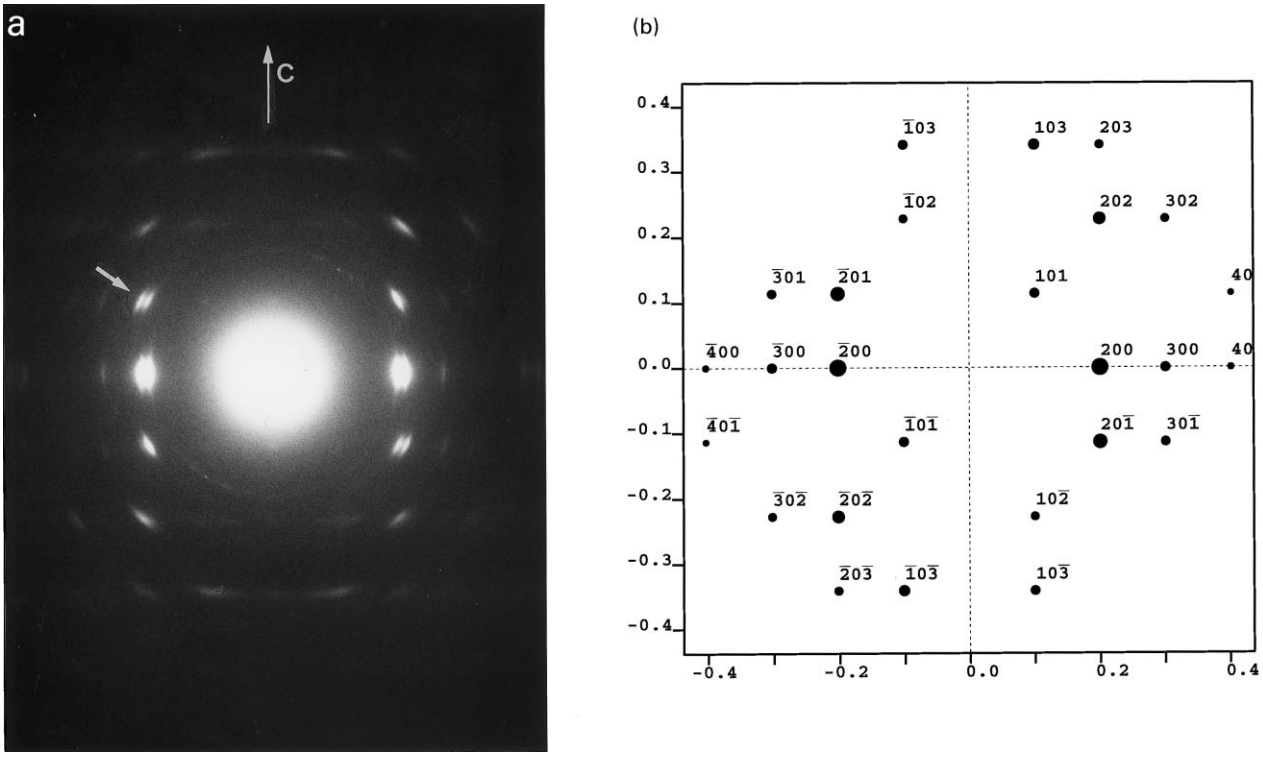

Fig. 2. (a) Electron diffraction pattern of a film of PLLA epitaxially crystallized on HMB crystals at 140°C. Chain axis vertical. Note the asymmetry of the pattern relative to the vertical "fiber" axis, as illustrated by the existence of the doublet on the first layer line (arrowed). (b) Indexation of part of the pattern in (a). The unit-cell is that shown in Fig. 4, and the zone axis is [0$\bar{1}$0], as illustrated in Fig. 5a. Note the asymmetry of the computed pattern, which matches that of the diffraction data in (a). The $\bar{2}$01 reflection corresponds to the outside reflection of the doublet arrowed in (a). Similar asymmetries are observed for *hhl* reflections, and accounted for by a selection of contact *faces* as illustrated in Fig. 5a.

pattern displays only rows of reflections indexed as 00*l*, 01*l* and 02*l*. The diffraction pattern is modeled in Fig. 1c. For the sake of completeness, Fig. 1d also shows a diffraction pattern (presented in previous papers [4,8]) of single crystals of this phase produced from solution. Fig. 1e shows a *c*-axis projection of the unit-cell, assuming a regular 10_7 helix conformation. This is only an approximation of the actual structure, which does not account for several features of both the epitaxially crystallized film and single crystal patterns (e.g. the prominence of a 010 reflection in Fig. 1d). Preliminary analyses (to be developed in a future work) suggest that the helix geometry is deformed, most probably "flattened" along the *b*-axis direction. Such deformations are observed for helical geometries of "loose" polymer chains that have a symmetry different from that of their crystallographic environment: an illustrative example is provided by the 7_2 helix of poly(ethylene oxide) in the nearly tetragonal environment of its monoclinic unit-cell [27]. This molecular asymmetry of PLLA explains the *selectivity* of the epitaxial relationship, which probably does not rest solely on a *dimensional matching* criterion. Indeed, the packing of PLLA helices in the unit-cell is very nearly hexagonal (cf. Fig. 1e and the four strong 110 and two 200 spots in the diffraction pattern of Fig. 1d). As a consequence, a similar *geometric* lattice match can be achieved when the contact plane is {110} rather than the (100) plane considered above: the interchain distances in these planes are equal to within 0.1 Å (0.61 versus 0.6115 nm). However, these values are valid for the room temperature cell parameters, i.e. disregarding possible differences linked with thermal expansion, since the epitaxy takes place at ≈160°C.

3.1.2. γ-Phase fiber pattern and epitaxy

When the epitaxial crystallization of PLLA takes place at lower temperatures (≈140°C) in the presence of HMB, a significantly different diffraction pattern is obtained (Fig. 2a). The much simpler layer line organization indicates at once a three-fold symmetry of the helix. Three-fold helical conformations are familiar for polylactides, since they are observed in the racemate structure, as well as in the form obtained upon stretching of the chiral α-form (the β-structure, to be analyzed in the companion paper [15]). While very similar to the diffraction patterns of the β-form obtained by Hoogsten et al. [2] and by Okihara et al. [4] (cf. also the companion paper), this pattern has however several original features which suggest that we are dealing with *a new crystal phase*, hereafter named the γ-phase. In particular, and in sharp contrast with the patterns of the β-phase, the first cluster of strong reflections on the equator is made of two reflections, which rules out hexagonal packing. These reflections have counterparts on the first and second layer lines. Note however, and this will be an essential ingredient of the structure derivation developed in the next section and of the analysis of the epitaxial relationship, that the pattern is *asymmetrical* relative to the chain axis direction. This asymmetry is most prominent for the doublet of reflections on the first layer arrowed in Fig. 2a, which have significantly different intensities on the other side of the meridian. This asymmetry also indicates that we are not dealing with a fiber pattern. Anticipating results of the crystal structure derivation developed later, this pattern indicates epitaxy with two contact planes, the *ac*-plane being the most prominent one. Indexation of the pattern with this crystal structure and contact plane is displayed in Fig. 2b.

3.1.3. Epitaxy of the racemate

Equimolecular mixtures of PLLA and PDLA epitaxially crystallized on HMB yield an oriented thin film of the racemate structure. The diffraction pattern (Fig. 3a) is consistent with the triclinic unit-cell and crystal structure derived by Okihara et al. [4] or with the equivalent, larger trigonal unit-cell suggested by Cartier et al. [8] (the latter cell, illustrated in Fig. 3c, will be used throughout this work). It is characterized by only few reflections: on the equator, 110 at spacing 7.49 Å (and its second order 220). These reflections indicate that the zone axis is $[1\bar{1}0]$. The viewing direction is therefore parallel to the double layers of right- and left-handed helices shown in Fig. 3c, and the contact plane is $(2\bar{1}0)$. Note, however, that this plane is structurally equivalent to the *ac* or *bc*-planes; for simplicity, the *ac* plane has been indicated as the contact plane in Fig. 3a. The reflections located on the first and second layer lines of Fig. 3a do not belong to this $[1\bar{1}0]$ zone axis: they are indexed as 211 and 012. They are, however, located near the diffracting planes and they become visible in this projection, probably as a result of a small tilt of the film (tilts of the *c* axis of 18 and 10°, respectively, would bring them in diffracting conditions). For this crystal phase also, we include (Fig. 3b) an *hk*0 diffraction pattern of chain-folded single crystals obtained by solution or thin-film crystallization [4].

3.2. Crystal structures of the various phases

The above experiments yield an unprecedented set of diffraction data on the various crystalline modifications of PLLA and the racemate, which can be the basis of extensive structural analyses. At this stage, particular attention has been focused on the structure of the racemate and that of the newly observed γ crystal phase.

3.2.1. Crystal structure of the racemate

The crystal structure of the racemate is clearly based on a three-fold helical structure, which has the same handedness as the helices of the α-phase: left-handed for PLLA and right-handed for PDLA. Furthermore, the structure is constrained by symmetry considerations, and rests on the body of evidence which has accumulated on crystal structures of isotactic polyolefins, poly(1-butene) in particular. In line with the work of Cartier et al. [8], the crystal structure is described in the $R3c$ or $R\bar{3}c$ space group, depending on the absence or existence of statistical up–down orientation of

Table 1
Fractional coordinates of the racemic phase of poly(D-L-lactide). Unit-cell parameters: $a = b = 14.98$ Å, $c = 8.8$ Å, $\alpha = \beta = 90°$, $\gamma = 120°$. Trigonal cell, assumed space group: *R*3*c* (all chains parallel)

Atom	*x*/*a*	*y*/*b*	*z*/*c*
C (H_3)	0.5074	0.3284	0.1536
C (H)	0.4251	0.3518	0.0918
C (=O)	0.3481	0.3355	0.2178
O (=C)	0.2689	0.2529	0.2329
O	0.3818	0.4211	0.3017

helices at each site. Packing of the six helices in the unit-cell is quite constrained by the symmetry operators and the requirement of absence of steric conflicts. Atomic coordinates of a structure with minimized packing energy are given in Table 1, the crystal structure is represented in Fig. 3c and the fiber pattern and indexing in Fig. 3d. Note that this pattern is fully consistent with the pattern of the epitaxially crystallized sample (which is not very informative however, on account of its paucity, since only one zone axis is involved), and with the published X-ray fiber patterns. As already indicated, the present data are also consistent with the crystal structure determined by Okihara et al. [4], based on a smaller, triclinic unit-cell with two enantiomorphous, antiparallel chains.

3.2.2. Crystal structure of the new γ-phase

The original diffraction pattern displayed in Fig. 2a has been interpreted as indicating the existence of a new crystal phase of PLLA, the γ-phase. This structure is now derived mainly by packing energy analysis based on the available diffraction evidence. Since this crystal structure turns out to resemble a structure proposed by Brizzolara et al. [5] for the "stretched" or β-phase of PLLA, the differences between the two models will be analyzed in detail.

As indicated earlier, the diffraction pattern of Fig. 2a has many features of a fiber pattern, but *it is not a fiber pattern*. The pattern does not correspond to a single zone axis either: the existence of several sets of *hk*0 (and corresponding *hkl*) diffraction spots, which might suggest fiber organization, arises from a mere circumstantial, albeit favorable feature, namely the coexistence of different contact planes. In other words, we are dealing with a combination of single crystal diffraction patterns, in which only a few (but by no means all) zone axes normal to the chain axis are imaged. It is nevertheless possible to derive the unit-cell geometry and crystal structure and actually take advantage of the (nearly) single crystal character of the pattern in this derivation.

All the reflections of the diffraction pattern can be accounted for if the first two strong equatorial reflections are indexed as 110 and 200 of an orthorhombic cell. The cell parameters are $a = 9.95$ Å, $b = 6.25$ Å, $c = 8.8$ Å, and the cell houses two three-fold helices.

The crystal structure derivation assumes the known three-fold helix of polylactides and rests on an extensive packing energy analysis. This analysis indicated early on that the structure must rest on an *antiparallel* orientation of the two helices in the unit-cell. As discussed in more detail in the next paper [15] in connection with the analysis of the

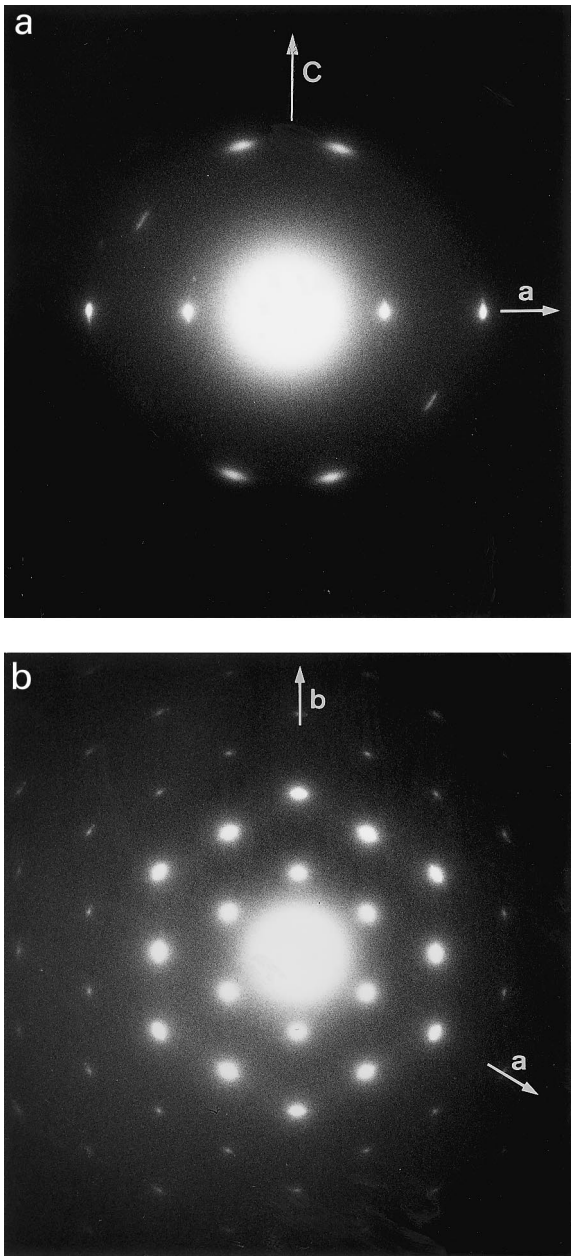

Fig. 3. (a) Electron diffraction pattern of a film of the racemic blend of PLLA and PDLA epitaxially crystallized on HMB. Chain axis vertical. (b) *hk*0 Electron diffraction pattern of a single crystal of the PLA racemate. a^*-axis horizontal. (c) Crystal structure of the PLA racemate obtained by packing energy minimization and using the experimentally determined unit-cell parameters deduced from parts (a) and (b). The trigonal cell is shown here made of parallel helices only, but statistical up–down orientation of helices is likely at any chain site (space group $R\bar{3}c$). The structure is made of alternating layers of right- and left-handed helices (i.e. of PDLA and PLLA molecules, respectively), and is similar to that of several isotactic polyolefins, e.g. isotactic poly(1-butene). (d) Computed fiber diffraction pattern of the structure shown in (c), with the corresponding indexing.

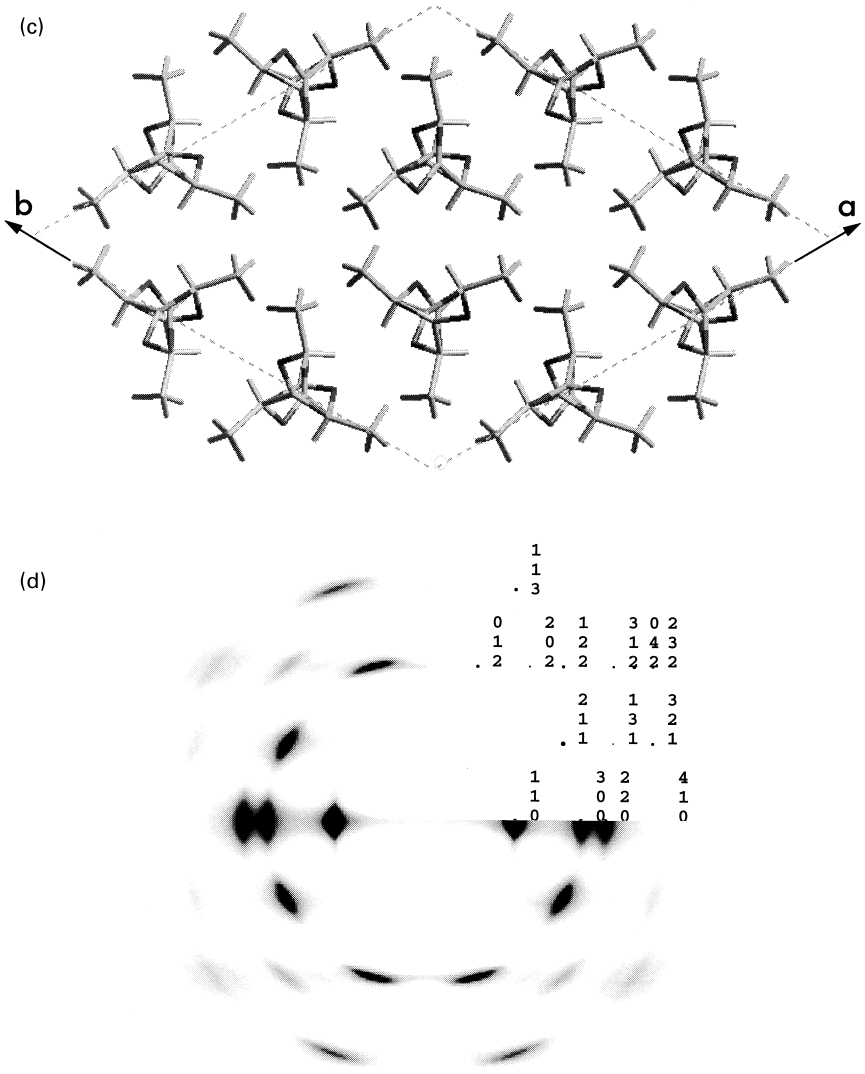

Fig. 3. (*continued*)

β-structure, the packing energy analysis indicates that *parallel* arrangement of helices leads to a trigonal, one chain unit-cell.

The crystal structure is shown in Fig. 4 (for convenience, as a centered cell). The computed cell dimensions are remarkably close to the experimental ones—less than 0.2 Å difference for the worst match (the *c* axis distance is kept at its experimentally determined value). The atomic coordinates are given in Table 2. The calculated diffraction intensities (computed fiber diffraction pattern in Fig. 4c) are also in good qualitative agreement with the observed ones. A quantitative analysis is not made since the experimental pattern is a combination of different "single crystal" patterns (associated with different contact planes), the relative proportions of which are not controlled. In spite of these limitations, the model may be considered as firmly supported by experimental evidence, in particular because it accounts for the curious asymmetry of the pattern underlined earlier. Indeed, the unit-cell is non-centrosymmetric

Table 2
Fractional coordinates of the γ-phase of poly(L-lactide). Unit-cell parameters: $a = 9.95$ Å, $b = 6.25$ Å, $c = 8.8$ Å, $\alpha = \beta = \gamma = 90°$. Monoclinic space group: $P2_1$ (#14), unique axis: *b*. Coordinates of the second chain: $-x$, $1/2 + y$, $-z$

Atom	*x*/*a*	*y*/*b*	*z*/*c*
C (H)	0.3820	0.5068	−0.1342
C (H_3)	0.5136	0.4105	−0.1960
O	0.3352	0.3809	−0.0108
C (=O)	0.2426	0.4735	0.0765
O (=C)	0.2020	0.6563	0.0614
C (H)	0.1882	0.3289	0.1923
C (H_3)	0.0699	0.1959	0.1305
O	0.1433	0.4565	0.3158
C (=O)	0.2399	0.5376	0.4030
O (=C)	0.3596	0.5021	0.3879
C (H)	0.1882	0.6848	0.5291
C (H_3)	0.1747	0.9143	0.4673
O	0.2801	0.6834	0.6525
C (=O)	0.2762	0.5095	0.7398
O (=C)	0.1971	0.3619	0.7247

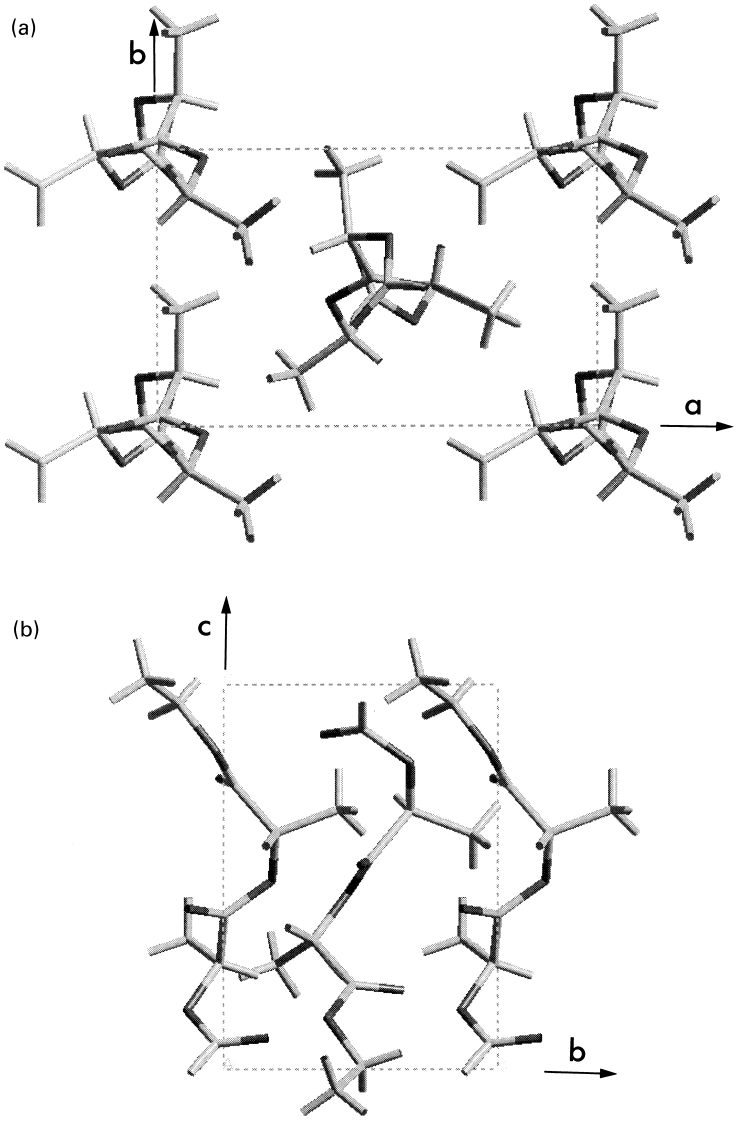

Fig. 4. (a) Chain axis projection and (b) *a*-axis projection of the crystal structure determined for the γ-phase of PLLA produced by epitaxial crystallization on HMB at 140°C. The structure corresponds to a minimum of the packing energy. The two antiparallel helices are linked by a 2_1 screw axis parallel to *b*. (c) Computed fiber diffraction pattern of the γ-phase of PLLA.

since we are dealing with a chiral polymer and three-fold helix conformation. As a consequence, *hkl* and $-h-kl$ reflection have similar spacings, but different intensities. These features are analyzed in more detail in the next section, in connection with the use of epitaxial crystallization in structure analysis.

To conclude this section, a short comment on the differences with the structure derived by Brizzolara et al. [5] is in order. Indeed, the crystal structure derived above is characterized by setting angles which are very reminiscent of those proposed by Brizzolara et al. [5] for the β-phase of PLLA. There are, however, some significant differences. As already indicated, the structure derived in the present work corresponds to a result of the packing energy minimization which fits the experimental unit-cell geometry (orthorhombic) and cell parameters. To the contrary, analysis of the work of Brizzolara et al. indicates that the cell dimensions were fixed rather arbitrarily, and correspond to a "scaling down" of the orthorhombic unit cell proposed by Hoogsten et al. [2] The model building was performed to fit that unit-cell, and is not therefore a minimized structure. Also, the relative chain orientation, which we consider as an essential ingredient in the formation of the γ-structure, was not considered in the same detail, and the structure described is made of parallel chains. Finally, as mentioned already, the structure derived by Brizzolara et al. [5] was designed to account for a different structure of PLLA, namely the β-phase, obtained on stretching the α-phase. As analyzed in the companion paper [15], this β-phase is characterized by a frustrated packing of chains which differs significantly from the antiparallel arrangement of chains considered here.

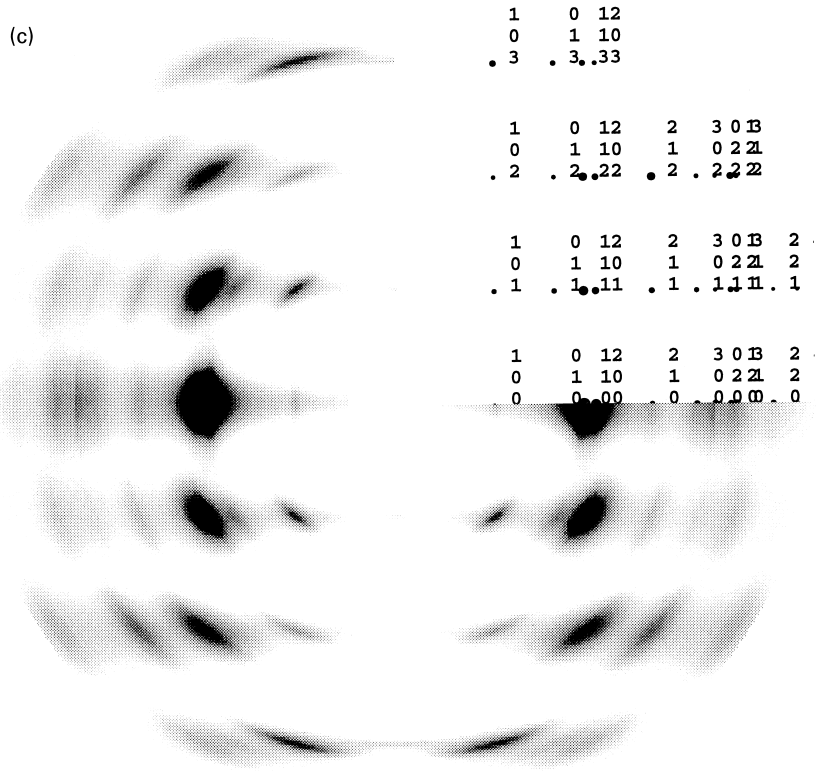

Fig. 4. (*continued*)

3.3. Epitaxy of chiral polymers

The two main features of the epitaxial crystallization of polylactides are: (a) the extreme versatility of HMB in inducing the different phases of PLA; and (b) the formation of a truly single crystal orientation of the new γ-phase, as attested by the asymmetry of its diffraction pattern.

The versatility of HMB as a substrate is difficult to analyze, in view of the fact that no composite diffraction patterns are available, due to the volatility of HMB in the vacuum of the electron microscope: its analysis will require further experiments with a cryo-stage. HMB has a triclinic unit-cell with parameters $a = 8.92$ Å, $b = 8.86$ Å, $c = 5.30$ Å, $\alpha = 44°27'$, $\beta = 116°43'$, $\gamma = 119°34'$, space group $P\bar{1}$ [12]. In the cell, the planes of the benzene rings are parallel to the *ab*-plane. It is of interest to note that both the HMB *a* and *b* parameters are close to the chain axis repeat distance of the polylactides in the 3_1 helical conformation, or even of the helical pitch of the 10_3 or 10_7 form (i.e. $28.8/3 = 9.4$ Å). Molecular modeling of the crystal habit shows that the most prominent faces are low index *hk*0 faces, i.e. the exposed faces include the *a* and/or *b* parameters: they offer a potential favorable match with the chain axis repeat of the polymer. This match is probably not the only one involved, since well-defined contact faces are selected for all three crystal forms. However, in the contact planes, interchain distances vary significantly (6.10, 15 Å (for a doublet of helices) and 9.95 Å for the α-racemate and γ-phases, respectively), which makes it difficult to analyze in detail the epitaxial relationships in the absence of definite experimental evidence (i.e. composite diffraction patterns) for each phase.

The second aspect deals with the observed asymmetries in intensity of the diffraction pattern observed for the γ-phase. As analyzed now, these asymmetries reflect the fact that the epitaxy selects one *face* of any crystallographic *plane* as the contact face.

Concentrating first on the *ac*-plane of this γ-phase (horizontal in Fig. 4a and illustrated schematically in Fig. 5a), it is clear that the *front* face (say, top) of the layer has a different topography than the *back* (bottom) face: the first is populated with methyl groups which stand nearly "erect" out of the face, whereas the second corresponds more or less to a base of the triangular projection of the three-fold helix. As a consequence, and even though we are dealing with identical dimensional match in the epitaxial relationship, one face may be favored as a contact face due to a more favorable surface topography. In other words also, the epitaxy discriminates between the $+b$ and the $-b$ axis, i.e. we are dealing with a true single crystal orientation. As a further consequence, all helices in the contact plane are *parallel* (as a result of the crystal symmetry) in any one "single crystal" domain, with boundaries between domains made of antiparallel chains (coexistence of such antiparallel domains maintains the asymmetry of the diffraction pattern). This single-crystal character makes it also possible *on the basis of diffraction evidence alone* (i.e. on the differences in intensity of corresponding reflections) to determine

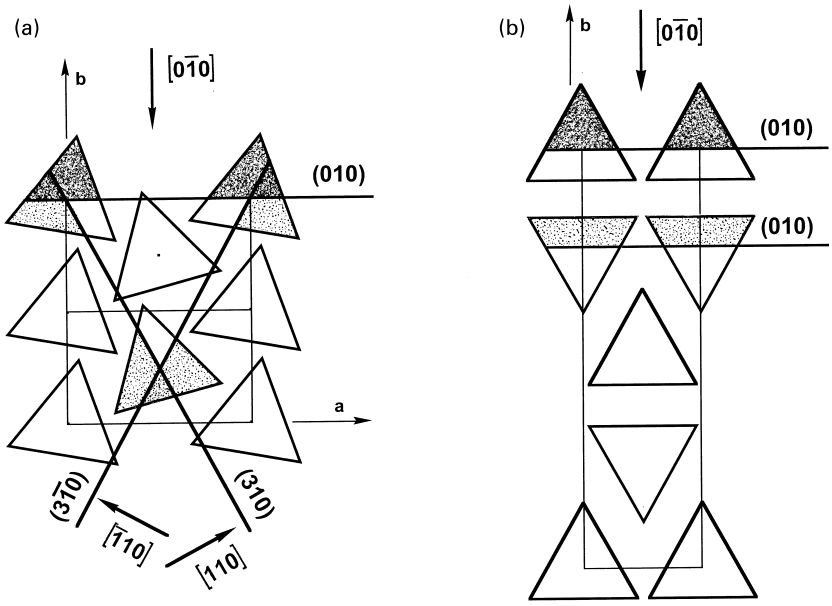

Fig. 5. (a) Illustration of the specificity of contact faces resulting from epitaxy of the γ-phase, giving rise to the diffraction pattern asymmetries of Fig. 2a. The helices are schematized by triangles, with the methyl group protruding out of the contact face being shaded in dark grey (most likely contact plane: ((010)) and in light grey ({110} contact planes). Observation of the contact faces *from the viewpoint of the substrate* results in a selection of viewing directions (shown by bold arrows): the (010) contact face is only observed from the $+b$-direction, *but not* from the $-b$ direction; thus the asymmetry of Fig. 2a. A similar reasoning applies for the {310} contact planes. The various zone axes are illustrated by bold arrows. The two viewing directions along {110} planes (bottom arrows) yield patterns with identical asymmetries. (b) The two potential (010) contact faces of isotactic polypropylene, α-phase: although the diffraction pattern is also asymmetric, two topographically different contact faces are possible (the actual one, determined by AFM, is shown in dark shading).

the exact contact face in the epitaxy. Experimentally, this requires of course a strict control of the sample orientation through all stages of the epitaxy and subsequent electron diffraction investigation.

The situation is very similar for the other set of reflections present in the diffraction pattern of Fig. 2a, namely the set of, say, 11*l* ones. Presence of these reflections indicates that the contact planes involved are {310} (Fig. 5a), which are again made up with second nearest-neighbor chains. The lattice match in the epitaxy is therefore nearly comparable to that in the (010) plane, in view of the near-hexagonal packing of the helices (interhelix distance: 10.6 Å, as opposed to 9.6 Å for (010)). However, the contact plane is structurally less regular since successive helices in the contact plane are antiparallel to each other. Nevertheless, two distinctly different contact surface types can again be recognized, which correspond roughly, on one hand, to methyl groups "sticking out" of the layer surface, and on the other, to methyl groups lying more "in" the layer surface. If the selection rule described above for the (010) contact surface also applies, only two structurally identical faces of the {310} planes should be contact planes: these are highlighted in Fig. 5a by the lightly shaded "tips". Again, if the epitaxy involves only this type of contact face, the film is observed only along the two zone axes shown in Fig. 5a. These equivalent zone axes yield patterns with similar asymmetries, and therefore account for the features of the diffraction pattern of these epitaxially crystallized films.

The issue of selection of a single contact *face* of a contact *plane* just developed has a close counterpart in the epitaxy of the (010) face of isotactic polypropylene (αiPP) on benzoic acid [28]. In the crystal structure of αiPP, three-fold helices are packed in layers parallel to the *ac* plane, in such a way that either one methyl group sticks out of the plane, or two methyl groups are in the exposed face. As shown in Fig. 5b, and due to the existence of a glide plane parallel to the *ac* plane, there are *two* possible, but different (010) contact planes for any *one* orientation of the unit-cell: the different exposed topographies are shown shaded. In this case, discrimination between the two possible contact planes is only possible by probing the contact face, i.e. by resorting to AFM imaging of the surface topography. The AFM investigation demonstrates that the face populated with methyl groups "sticking out" is the contact face (dark shading in Fig. 5b) [28]. In the PLLA case on the contrary, discrimination can be made on the sole basis of the diffraction pattern, since the polymer is chiral and the unit-cell symmetry does not generate the same ambiguity as encountered in αiPP.

Although rather involved, these analyses emphasize the usefulness of epitaxial crystallization in polymer structure analysis. As illustrated here, the epitaxial interactions can discriminate between two structurally different faces of the same crystallographic plane, thus providing a means to generate a truly single crystalline texture. This is in sharp contrast with more conventional (usually mechanical)

orienting methods, which generate mostly fiber or at best biaxial orientation.

4. Conclusion

Polylactides in either enantiomeric or racemic forms crystallize epitaxially on HMB, a low molecular weight organic solvent that had been shown by Zwiers et al. [11] to form eutectics with the polymer. Epitaxial crystallization of polymers associated with eutectic formation in binary low molecular weight organic solvent/polymer systems has already been documented in a number of cases [13,14]. However, the original feature revealed by the present study is that *three* different crystal phases of PLAs can be epitaxially crystallized on one and the same substrate: the racemate, and the enantiomer in its conventional α-form as well as in a novel γ-form based on a three-fold helix conformation. This versatility probably arises from the fact that a major constituent of the epitaxial matching involves the chain axis repeat (or the helical pitch for the α-phase) which are always close to 8.8–9 Å. The new γ-phase structure analyzed in the present paper is characterized by *strict antiparallelism* of the two chains which build up the unit-cell. This structure has been observed so far only as a result of epitaxial crystallization. Specific as it may be, it turns out to be of considerable help in the analysis of the better known β-phase of polylactide obtained on mechanical stretching, which is described in the companion paper [15].

Acknowledgements

Special thanks are due to the Spanish Secretaria de Estado de Universidades, Investigación y Desarrollo for supporting the stay of G.P. in Strasbourg.

References

[1] De Santis P, Kovacs A. J Biopolym 1968;6:299.
[2] Hoogsten W, Postema AR, Pennings AJ, tenBrinke G, Zugenmaier P. Macromolecules 1990;23:634.
[3] Eling B, Gogolewski S, Pennings AJ. Polymer 1982;23:1587.
[4] Okihara T, Tsuji M, Kawagushi A, Katayama KI, Tsuji H, Hyon SH, Ikada Y. J Macromol Sci Phys B 1991;30:119.
[5] Brizzolara D, Cantow HJ, Diederichs K, Keller E, Domb AJ. Macromolecules 1996;29:191.
[6] Ikada Y, Jamshidi K, Tsuji H, Hyon SH. Macromolecules 1987;20:904.
[7] Okihara T, Kawaguchi A, Tsuji H, Hyon S-H, Ikada Y, Katayama K. Bull Inst Chem Res Kyoto Univ 1988;66:271.
[8] Cartier L, Okihara T, Lotz B. Macromolecules 1997;30:6313.
[9] Natta G, Corradini P, Bassi IW. Nuovo Cimento 1960;15(1):52 (suppl.).
[10] Natta G, Corradini P, Bassi IW. Nuovo Cimento 1960;15(1):69 (suppl.).
[11] Zwiers RJM, Gogolewski S, Pennings AJ. Polymer 1983;24:167.
[12] Brockway LO, Robertson JM. J Chem Soc, Part II 1939:1324.
[13] Wittmann JC, St John Manley R. J Polym Sci Polym Phys 1977;15:1089.
[14] Wittmann JC, Hodge AM, Lotz B. J Polym Sci Polym Phys Ed 1983;21:2495.
[15] Puiggali J, Ikada Y, Tsuji H, Cartier L, Lotz B. Polymer 2000;41:8921–8930.
[16] Lotz B, Kopp S, Dorset DL. C R Acad Sci 1994;319:187.
[17] Cartier L, Spassky N, Lotz B. C R Acad Sci, Ser II b 1996;322:429.
[18] Lotz B, Cartier L, Okihara T, Puiggali J. Polym Prepr Polym Mater Sci Engng 1999;81:228.
[19] Sorenson WR, Campbell TW, editors. Preparative methods of polymer chemistry New York: Wiley, 1961.
[20] Tsuji H, Horii F, Hyon S-H, Ikada Y. Macromolecules 1991;24:2719.
[21] Tsuji H, Hyon S-H, Ikada Y. Macromolecules 1991;24:5651.
[22] Tsuji H, Hyon S-H, Ikada Y. Macromolecules 1991;24:5657.
[23] Tsuji H, Hyon S-H, Ikada Y. Macromolecules 1992;25:2940.
[24] Tsuji H, Hyon S-H, Ikada Y. Macromolecules 1992;25:5719.
[25] Tsuji H, Ikada Y. Macromolecules 1993;26:6918.
[26] Wittmann JC, Lotz B. Prog Polym Sci 1990;15:909.
[27] Tadokoro H. Structure of crystalline polymers. New York: Wiley, 1980.
[28] Stocker W, Magonov SN, Cantow HJ, Wittmann JC, Lotz B. Macromolecules 1993;26:5915 (Correction 1994;27:6690).